Effect of alkylglycerone phosphate synthase on the expression levels of lncRNAs in glioma cells and its functional prediction

LEI CHEN[1*], WEIJIAN ZHANG[2*], LIHUA HE[2,3], LI JIN[4], LIYU QIAN[5] and YU ZHU[6]

[1]Department of Otolaryngology, The Second Hospital of Tianjin Medical University, Tianjin 300211; [2]Postgraduate School of Tianjin Medical University, Tianjin 300070; [3]Department of Clinical Laboratory, Affiliated Hospital of Hebei University of Engineering, Handan, Hebei 056002; [4]Integrated Chinese and Western Medicine School of Tianjin University of Traditional Chinese Medicine, Tianjin 301617; [5]Department of Tumor Surgery, The First Affiliated Hospital of Bengbu Medical College, Bengbu, Anhui 233004; [6]Department of Clinical Laboratory, Tianjin Haihe Hospital, Tianjin 300350, P.R. China

Received December 5, 2019; Accepted May 18, 2020

DOI: 10.3892/ol.2020.11927

Abstract. Alkylglycerone phosphate synthase (AGPS) is a key enzyme for ether ester synthesis and acts as an oncogene in malignant tumors. The present study aimed to investigate the effect of AGPS silencing on the expression levels of long non-coding RNAs (lncRNAs) and the co-expression with mRNAs in glioma U251 cells using microarray analysis. Furthermore, the underlying biological functions of crucial lncRNAs identified were investigated. It was discovered that *in vitro* U251 cell proliferation was suppressed following the genetic silencing of AGPS. Differentially expressed lncRNAs and mRNAs in U251 cells were sequenced following AGPS silencing. The results from the Gene Ontology analysis identified that the co-expressed mRNAs were mainly involved in biological processes, such as 'cellular response to hypoxia', 'extracellular matrix organization' and 'PERK-mediated unfolded protein response'. In addition, Kyoto Encyclopedia of Genes and Genomes signaling pathway enrichment analysis revealed that the co-expressed mRNAs were the most enriched in the 'AGE/RAGE signaling pathway in diabetic conditions'. Additionally, the PI3K/Akt and epidermal growth factor receptor signaling pathways serve important roles in tumor processes, for example carcinogenesis and angiogenesis. Furthermore, it was identified that the lncRNA AK093732 served a vital role in the regulatory network and the core pathway in this network regulated by this lncRNA was discovered to be the 'Cytokine-cytokine receptor interaction'. In conclusion, the findings of the present study suggested that AGPS may affect cell proliferation and the degree of malignancy. In addition, the identified lncRNAs and their co-expressed mRNAs screened using microarrays may have significant biological effects in the occurrence, development and metastasis of glioma, and thus may be novel markers of glioma.

Correspondence to: Professor Yu Zhu, Department of Clinical Laboratory, Tianjin Haihe Hospital, 890 Jingu Road, Jinan, Tianjin 300350, P.R. China
E-mail: zhuyutj@126.com

Dr Lei Chen, Department of Otolaryngology, The Second Hospital of Tianjin Medical University, 23 Pingjiang Road, Hexi, Tianjin 300211, P.R. China
E-mail: clchenlei2008@163.com

*Contributed equally

Key words: glioma, long non-coding RNA, bioinformatics analysis

Introduction

Gliomas are the most common type of primary central nervous system tumor and intracranial malignant tumor, accounting for ~81% of all malignant brain tumors (1). Alkylglycerone phosphate synthase (AGPS) is an important enzyme for ether ester synthesis and it has been discovered to serve an important role in the pathogenicity of cancer cells (2). It was previously reported that the overexpression of AGPS increased the survival, migratory, proliferative and invasive abilities of tumor cells, including SKOV3 ovarian cancer, 231MFP breast cancer, C8161 melanoma, PC3 prostate cancer and primary breast cancer cells (3,4). Furthermore, the levels of tumor-related lipids, including ether lipids, prostaglandins and acyl phosphatides, were discovered to decrease following the inactivation of AGPS, resulting in a decrease in the cancer pathogenicity (5,6). In addition, our previous study revealed a positive correlation between AGPS and the malignant potential of gliomas (7). Therefore, it was hypothesized that the overexpression of AGPS may be an important mechanism for the aggravation of gliomas.

The present study analyzed changes in the expression profiles of long non-coding RNAs (lncRNAs) and co-expressed mRNAs in glioma. lncRNAs are RNAs of >200 nucleotides in length, which have no protein-coding ability due to the lack of a complete open reading frame (8). lncRNAs have been identified to regulate gene expression via a variety of biological processes, demonstrating important roles in the apoptosis, proliferation, invasion and metastasis of cells (9).

Moreover, mRNAs encode the genetic information for their corresponding protein (10). In the present study, the full-length sequence expression data for glioma cells was obtained using gene chip technology, and lncRNA and mRNA expression profiles from glioma cells were analyzed. In addition, their functions were predicted using bioinformatical methods, which provided a theoretical basis for studying the molecular mechanisms of the AGPS-induced malignancy, migration and invasiveness of glioma.

Materials and methods

Cell culture and AGPS short hairpin (sh)RNA lentivirus infection. U251 cells were obtained from the Cell Resource Center of the Chinese Academy of Medical Sciences. Cells were cultured in RPMI-1640 medium (Corning Life Sciences), supplemented with 10% FBS (Corning Life Sciences), and maintained in a CO_2-controlled incubator at a constant temperature of 37˚C.

For transfection, $2x10^5$ U251 cells were plated into a six-well plate with 2 ml medium/well the day before transfection and cultured at 37˚C for 24 h to reach 60-80% confluence on the second day. AGPS shRNA lentiviral particles (shR-AGPS-1 and -2 groups; Santa Cruz Biotechnology, Inc.) or empty lentiviral particles used as a negative control (control group; Santa Cruz Biotechnology, Inc.) stably integrated cell lines were established following infection with 8 μg/ml lentiviruses of U251 cells using 5 μg/ml polybrene-containing RPMI-1640 medium. After infecting the cells at 37˚C for 24 h, the medium was replaced with 2 ml RPMI-1640 medium without polybrene, and the cells were further incubated at 37˚C for 72 h. Cell morphology was observed under an inverted light microscope (magnification, x100 and x200).

Monoclonal cell selection. Following infection and further cell culture for 72 h, 1 mg/ml puromycin (5 μl; Beyotime Institute of Biotechnology) was added in the RPMI-1640 medium to the cells at 80% confluence. The RPMI-1640 medium with puromycin was refreshed every 3 days for 12 days. The cells in each group were separately diluted in RPMI-1640 medium via serial dilution to produce a single cell suspension with a density of $1x10^3$ cells/ml, which were subsequently plated into the first row of wells in a 96-well plate at 0.2 ml/well. From those first wells, 0.1 ml cell solution was inoculated into the second row and the process was then repeated until the 8th row, with the goal of ultimately obtaining wells containing single cells. Isolated cells were cultured at 37˚C for 1 week in complete medium to obtain monoclonal cell lines.

Cell proliferation assay. In total, $3x10^3$ cells/well were seeded into a 96-well plate and cultured at 37˚C for 24, 48 and 72 h. Cell proliferation was analyzed using a BrdU cell proliferation ELISA kit (cat. no. ab126556; Abcam), according to the manufacturer's protocol. Briefly, at each time point, 20 μl BrdU label was added and incubated at 37˚C for 12 h. Following the incubation, the cells were fixed with 3.7% formaldehyde diluted in PBS at room temperature for 30 min and then washed three times with PBS. Then, 100 μl anti-BrdU monoclonal detector antibody (1:2,000; supplied in the BrdU cell proliferation kit) was incubated with the cells for 1 h at room temperature. Following the incubation, each well was washed three times using PBS and 100 μl horseradish peroxidase (HRP)-conjugated goat anti-mouse IgG antibody (1:2,000; supplied in the BrdU cell proliferation kit) was added and incubated for 30 min at room temperature. The wells were washed three times with PBS and then, 100 μl 3,3,5',5'-Tetramethyl benzidine peroxidase substrate was added and incubated for 30 min at room temperature in the dark. Finally, 100 μl stop solution (supplied in the BrdU cell proliferation kit) was added and the optical density value was measured every 24 h using the Multiskan™ Spectrum microplate photometer (Thermo Fisher Scientific, Inc.) at 450 nm.

Western blotting. The selected stable U251 cell line ($2x10^5$ cells/well) was plated into a six-well plate and after 24 h, total protein was extracted using 300 μl/well RIPA lysis buffer (Beyotime Institute of Biotechnology). Cells were gently agitated at 4˚C for 30 min and then the cell lysate was transferred to a 1.5 ml centrifuge tube for centrifugation at 10,000 x g for 10 min at 4˚C. Total protein was quantified using a bicinchoninic acid assay, and 50 μg protein/lane was separated via 10% SDS-PAGE. The separated proteins were subsequently transferred onto a PVDF membrane and the membrane was blocked with 5% milk at room temperature for 2 h. The membrane was cut around the position of the protein according to the molecular size and then it was incubated with an anti-AGPS antibody (1:1,000; cat. no. sc-374201; Santa Cruz Biotechnology, Inc.) or an anti-β-tubulin antibody (1:1,000; cat. no. SRP01044; Saierbio, LLC) at 4˚C overnight. Following the primary antibody incubation, the membranes were washed 4 times for 5 min each with TBS-Tween (TBST; 0.5% Tween 20) solution and incubated with a HRP-conjugated goat anti-mouse IgG antibody (1:1,000; cat. no. SRPGAM001; Saierbio, LLC) or an HRP-conjugated goat anti-rabbit IgG antibody (1:1,000; cat. no. SRPGAR001; Saierbio, LLC) at room temperature for 1.5 h. The membranes were then washed and shaken in TBST solution 4 times for 5 min each. Total protein was visualized using a Western Lightning™ chemiluminescent agent (PerkinElmer, Inc.). The protein expression levels were analyzed using ImageJ Software v1.52 (National Institutes of Health) and the gray value for the AGPS band in each sample was normalized to the corresponding β-tubulin band. The control group was set at a standard value of 1 and a histogram was generated to compare all groups.

Screening to identify differentially expressed lncRNAs and co-expressed mRNAs. Total RNA was extracted from cells using the RNAeasy™ Animal RNA Isolation kit according to the manufacturer's protocol (Beyotime Institute of Biotechnology), and the QuantiTect Whole Transcriptome kit (Qiagen China Co., Ltd.) was used for library construction and amplification according to the manufacturer's protocol. The GeneChip Scanner 3000 System (Affymetrix; Thermo Fisher Scientific, Inc.) was used to detect the expression levels of lncRNA and the profile of co-expressed mRNAs using the Affymetrix Clariom D array in each group of cells. The control group and the two experimental groups were compared to screen differentially expressed lncRNAs and co-expressed mRNAs. The screening was analyzed using the free online

Table I. Primer sequences used for the reverse transcription-quantitative PCR.

Gene	Primer sequence (5'→3')
COL1A2	F: GTGCGATGACGTGATCTGTGA
	R: GTTTCTTGGTCGGTGGGTG
COL6A3	F: TCTGTTCCTCTTTGACGGCT
	R: CCACCTTGACATCATCGCTG
THBS1	F: GCTCCAGCTCTACCAATGTCCT
	R: TTGTGGCCGATGTAGTTAGTGC
FN1	F: CAGTGGGAGACCTCGAGAA
	R: TCCCTCGGAACATCAGAAAC
SPP1	F: TTCTCAGCCAAACGCCGA
	R: GGTAGGTACATCTTTAGTGCTGCTT
ITGA11	F: GTATTTGTAGGTTTTTTTGGATTGATTGT
	R: ATCCCTATTTAAAATACACACAAAAATTTC
VEGFA	F: GAGGGCAGAATCATCACGAAG
	R: TGTGCTGTAGGAAGCTCATCTCTC
IGF1R	F: GTGGAGACAGGGGCTTTTATT
	R: CTCCAGCCTCCTTAGATCACA
EGFR	F: CCTATGTGCAGAGGAATTATGATCTTT
	R: CCACTGTGTTGAGGGCAAT
TLN2	F: CTGAGGCTCTTTTCACAGCA
	R: CTCATCTCATCTGCCAAGCA
PXN	F: GCCCCTCTCAGAGCCTTTTC
	R: GCAGCTACTGAGGTCACAGC
AKT3	F: CCACAGGTCGCTACTATGCC
	R: ACAGCCCGAAGTCCGTTATC
PIK3CA	F: CATCATTTGCTCCAAACTGACCA
	R: CCTATGCAATCGGTCTTTGCC
JUN	F: AAGTGAAAACCTTGAAAGCTCAG
	R: TTAACGTGGTTCATGACTTTCTG
SHC3	F: AAAAAGCTTATGAGTGCCACCAGGAAGA GCCGG
	R: TTGGATCCCGGGGTTTCCTCTCCACTGGTT
FGF2	F: GAGAAGAGCGACCCTCACA
	R: TAGCTTTCTGCCCAGGTCC
ANGPT2	F: ACAGCAGAATGCAGTACAGAACCAGACG
	R: CAAGTCTCGTGGTCTGATTTAATACTTGG GCT
CSF3	F: CTGCTCTAGTGGACACACAAATG
	R: TTTCTCCGGACTAGGCTTTG
IL7R	F: AACCCCGTCTCCACTGAAAA
	R: GAGTCTTGCTTTGTTGCCCA
PRKAA2	F: GAAGATCGGACACTACGTGCT
	R: AACTGCCACTTTATGGCCTG
DDIT4	F: GGACCAAGTGTGTTTGTTGTTTG
	R: CACCCACCCCTTCCTACTCTT
HSP90B1	F: AAATCATTTTCAAAGGAAAGTGATGACCC
	R: CATCAAACAGACCACGTGGAGGAG
CREB5	F: ATTGACTCACCACCCTGCTG
	R: GCATGAAGGTGGGAATGGGA
TLR3	F: GCTCTGGAAACACGCAAACC
	R: CTCGTCAAAGCCGTTGGACT
IL1B	F: GGACAGGATATGGAGCAACAAGTGG
	R: TTCAACACGCAGGACAGGTACAGAT
CXCL8	F: TCAGAGACAGCAGAGCACAC
	R: ACACAGTGAGATGGTTCCTTCC
PTGS2	F: ATTGTACCCGGACAGGATTCTATG
	R: TTTGGAGTGGGTTTCAGAAATAATT
SDC4	F: ACCAGACGATGAGGATGTAGTG
	R: AAGGGATGGACAACTTCAGGG
β-actin	F: CTACAATGAGCTGCGTGTG
	R: AAGGAAGGCTGGAAGAGTGC

F, forward; R, reverse.

platform OmicShare tools (www.omicshare.com/tools), and the criteria were fold-change (|FC|)>1.2, P<0.05 and a false discovery rate <0.05.

Reverse transcription-quantitative PCR (RT-qPCR). Total RNA was extracted from cells using QIAzol reagent (Qiagen, Inc.) and reverse transcribed at 50˚C for 15 min using the BeyoFast™ Probe One-Step qRT-PCR kit (Beyotime Institute of Biotechnology), according to the manufacturer's protocol. To determine the expression levels of mRNAs, qPCR was subsequently performed using SYBR Green I dye (Takara Biotechnology Co., Ltd.) on a 7500 Real-Time PCR system (Applied Biosystems; Thermo Fisher Scientific, Inc.). The sequences of the primers used for the qPCR are listed in Table I. The following thermocycling conditions were used for the qPCR: Initial denaturation at 95˚C for 10 min, followed by 40 cycles at 95˚C for 15 sec and 60˚C for 60 sec, and a final extension step at 72˚C for 5 min. The expression levels of mRNAs were quantified using the $2^{-\Delta\Delta Cq}$ method (11) and normalized to the internal loading control β-actin.

Functional prediction of lncRNA and mRNA co-expression. The mRNAs co-expressed with the lncRNAs were subjected to functional term enrichment analysis using the Gene Ontology (GO) resource (http://geneontology.org), functional annotation of the differentially expressed genes and Venn diagrams were performed using free online platform OmicShare tools (www.omicshare.com/tools). Signaling pathway enrichment analysis was also performed on the co-expressed mRNAs using the Kyoto Encyclopedia of Genes and Genomes (KEGG) database (www.genome.jp) and the signaling pathways associated with the differentially expressed mRNAs were identified. Subsequently, Degree values were calculated using the OmicShare tools 3.0, and pathway networks and global signal transduction networks of co-expressed lncRNAs and mRNAs in AGPS-silenced U251 cells were constructed using the OmicShare tools with more connections there were, the higher the Degree. The differentially co-expressed lncRNAs and mRNAs predicted by GO functional term for biological process (BP) and KEGG signaling pathway enrichment analysis were used to determine the function of the unknown lncRNAs. The threshold of the Degree value was 1.

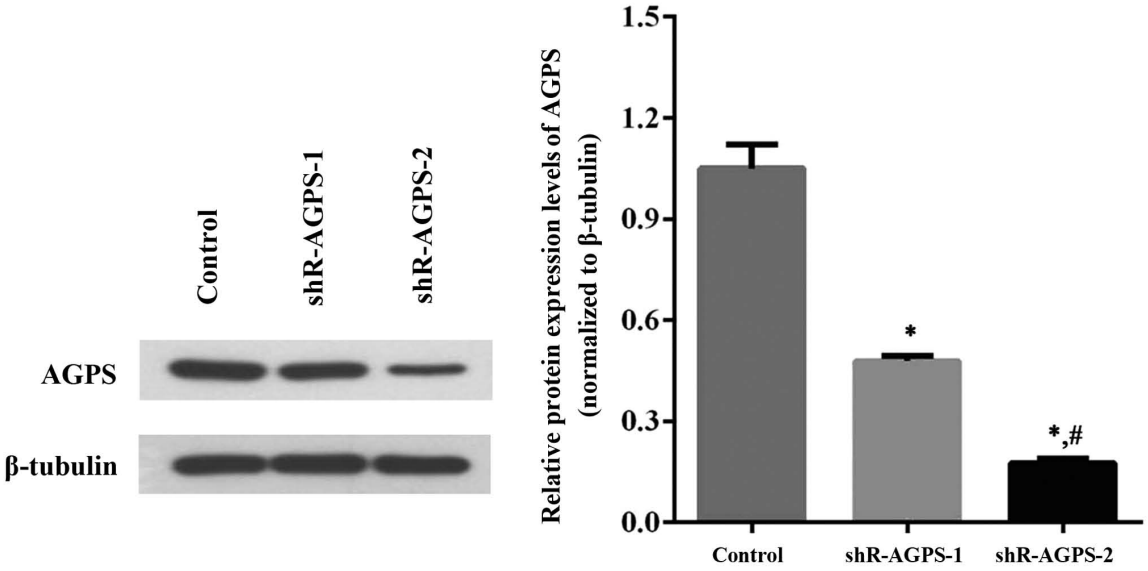

Figure 1. Effect of AGPS silencing on the expression levels of AGPS in glioma cells. Western blotting identified significantly downregulated expression levels of AGPS in AGPS-silenced U251 cells. n=3 *P<0.05 vs. control; #P<0.05 vs. shR-AGPS-1 group. shR, short hairpin RNA; AGPS, alkylglycerone phosphate synthase.

Statistical analysis. Statistical analysis was performed using SPSS version 11 software (SPSS, Inc.). Statistical differences were determined using a one-way ANOVA, followed by a Tukey's post hoc test for multiple group comparisons. P<0.05 was considered to indicate a statistically significant difference. A log10(P-value)>2 was considered to indicate a significant threshold for GO analysis.

Results

Effect of AGPS shRNA interference on AGPS expression levels in U251 cells. Two shR-AGPS lentiviral plasmids were transfected into U251 cells to construct stable AGPS-silenced U251 cell lines; negative control lentiviruses transfected into U251 cells were used as the control. In total, two groups (shR-AGPS-1 and shR-AGPS-2 group) of AGPS-silenced cell lines were established by monoclonal selection, and the AGPS expression levels in these shR-AGPS-1 and shR-AGPS-2 groups were significantly downregulated compared with the control group (Fig. 1). Furthermore, the expression levels of AGPS in the shR-AGPS-2 group were significantly downregulated compared with the shR-AGPS-1 group (Fig. 1).

Effect of AGPS silencing on the morphology of U251 cells. After silencing the expression levels of AGPS in U251 cells, the proliferation of each group was observed under a microscope at x100 and x200 magnification. The cell morphology of the shR-AGPS-1 and shR-AGPS-2 groups was observed (Fig. 2A). In addition, the proliferative ability in the shR-AGPS-2 group was significantly decreased compared with that in the shR-AGPS-1 and control groups after 48 and 72 h (Fig. 2B).Cluster analysis and regulation of differentially expressed lncRNAs and mRNAs. In the heatmap, the identified downregulated lncRNAs (107 for shR-AGPS-1 vs. control, 231 for shR-AGPS-2 vs. control, and 134 for shR-AGPS-1 vs. shR-AGPS-2) and mRNAs (61 for shR-AGPS-1 vs. control, 344 for shR-AGPS-2 vs. control,

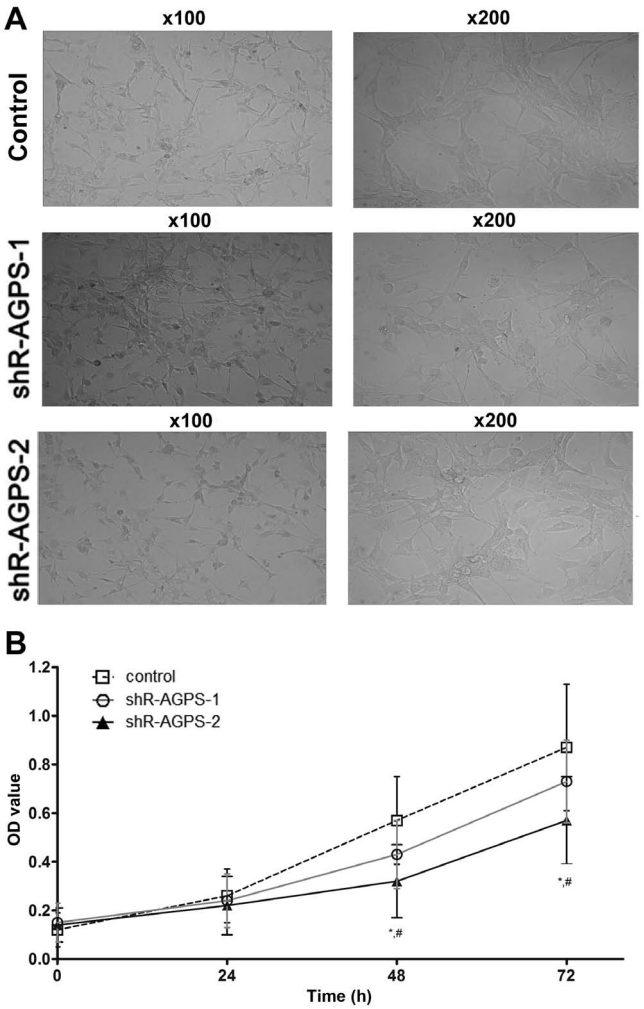

Figure 2. Effect of AGPS silencing on the cellular morphology of U251 cells. (A) Morphological observation under the microscope in AGPS-silenced U251 cells. Magnification, x100 or x200. (B) BrdU assay results revealed a significant inhibition over the proliferation of AGPS-silenced U251 cells. n=10. *P<0.05 shR-2 vs. shR-1, #P<0.05 shR-1 vs. control. shR, short hairpin RNA; AGPS, alkylglycerone phosphate synthase; OD, optical density.

Table II. Top 40 differentially expressed lncRNAs in AGPS-silenced human glioma U251 cells.

A, Top 40 differentially expressed lncRNAs in the shR-AGPS-1 vs. control groups

lncRNA	Upregulated FC	lncRNA	Downregulated FC
LINC00837	1.79	CR604135	1.32
CR626472	1.49	CTC-436K13.3	1.76
ERI3-IT1	1.48	AK129941	1.64
linc-AKR1B10-2	1.44	MIR548AA2	1.58
AF344193	1.44	linc-FCGR1B-7	1.57
LINC01079	1.41	AK098597	1.42
XXbac-B33L19.4	1.41	AF086041	1.40
ENST00000551732	1.40	linc-LOC388630-3	1.40
AC008440.10	1.40	linc_luo_384	1.40
linc_luo_541	1.39	linc-SEC23B	1.39
linc-TMEM169-2	1.35	linc-CNTN3-3	1.39
linc-MAGEA1-1	1.35	linc-TEKT4-1	1.39
AF087965	1.34	uc003srb.1	1.38
LOC101928354	1.34	BX641068	1.38
FENDRR	1.34	linc_luo_692	1.36
CR618740	1.33	uc011edo.1	1.35
linc-ZFP42-2	1.33	LINC00973	1.34
linc-B4GALT1	1.32	FAM138B	1.34
BC047484	1.31	LUCAT1	1.33
AK054755	1.29	linc-ERG-8	1.33

B, Top 40 differentially expressed lncRNAs in the shR-AGPS-2 vs. control groups

lncRNA	Upregulated FC	lncRNA	Downregulated FC
LINC00837	2.95	CR618823	2.59
FENDRR	2.21	MIR548AA2	2.58
linc-U2AF1-1	1.71	LINC00973	2.42
CTD-2377D24.4	1.66	linc_luo_1251	2.11
LOC100506532	1.56	LINC00263	2.01
FENDRR	1.55	linc-JAK1-1	1.95
CR624806	1.55	BC013423	1.88
AK130416	1.50	linc-COL1A2-2	1.87
linc-ARHGAP11B-2	1.47	linc_luo_1846	1.85
uc004cic.2	1.46	linc-WDR7-7	1.83
AF344193	1.46	AC003092.1	1.82
AF147353	1.45	uc001tkz.2	1.81
linc-UMODL1-5	1.44	linc_luo_1223	1.79
linc-AKR1B10-2	1.44	AL110176	1.78
linc-SLC16A7-1	1.42	LUCAT1	1.76
ERI3-IT1	1.42	CTC-436K13.3	1.76
linc-CDH11-5	1.42	uc003flo.2	1.7
AL133249.1	1.4	uc001gla.1	1.69
ENST551732	1.4	FAM138B	1.66
AC008440.10	1.4	uc003cpd.1	1.65

Table II. Continued.

C, Top 40 differentially expressed lncRNAs in the shR-AGPS-1 vs. shR-AGPS-2 groups

lncRNA	Upregulated FC	lncRNA	Downregulated FC
FENDRR	1.65	CR618823	1.97
LINC00837	1.65	LINC00973	1.80
CTD-2377D24.4	1.62	BC013423	1.79
linc-U2AF1-1	1.61	LINC00263	1.70
linc-LRRC8D-1	1.53	AL110176	1.69
linc-ACVR2B	1.47	linc_luo_1223	1.64
linc-GPATCH2-4	1.46	MIR548AA2	1.63
AF147353	1.45	linc-WDR7-7	1.62
linc-FBRSL1-3	1.44	linc_luo_1251	1.61
LINC01314	1.44	uc002axu.2	1.58
linc-UMODL1-5	1.44	uc001tkz.2	1.57
linc-SLC16A7-1	1.42	linc_luo_888	1.53
linc-RREB1-2	1.42	AX721161	1.53
linc-CDH11-5	1.42	linc-COL1A2-2	1.53
linc-PELO-3	1.40	linc-PTPRQ-4	1.50
linc-GADD45G-1	1.40	CR598627	1.50
linc-COX4NB-1	1.39	AL833129	1.49
RP11-339N8.1	1.38	uc003hoi.2	1.49
linc-SIPA1L1	1.38	CR626472	1.49
U84508	1.37	uc003cpd.1	1.49

lncRNA, long non-coding RNA; FC, fold change; shR, short hairpin RNA; AGPS, alkylglycerone phosphate synthase.

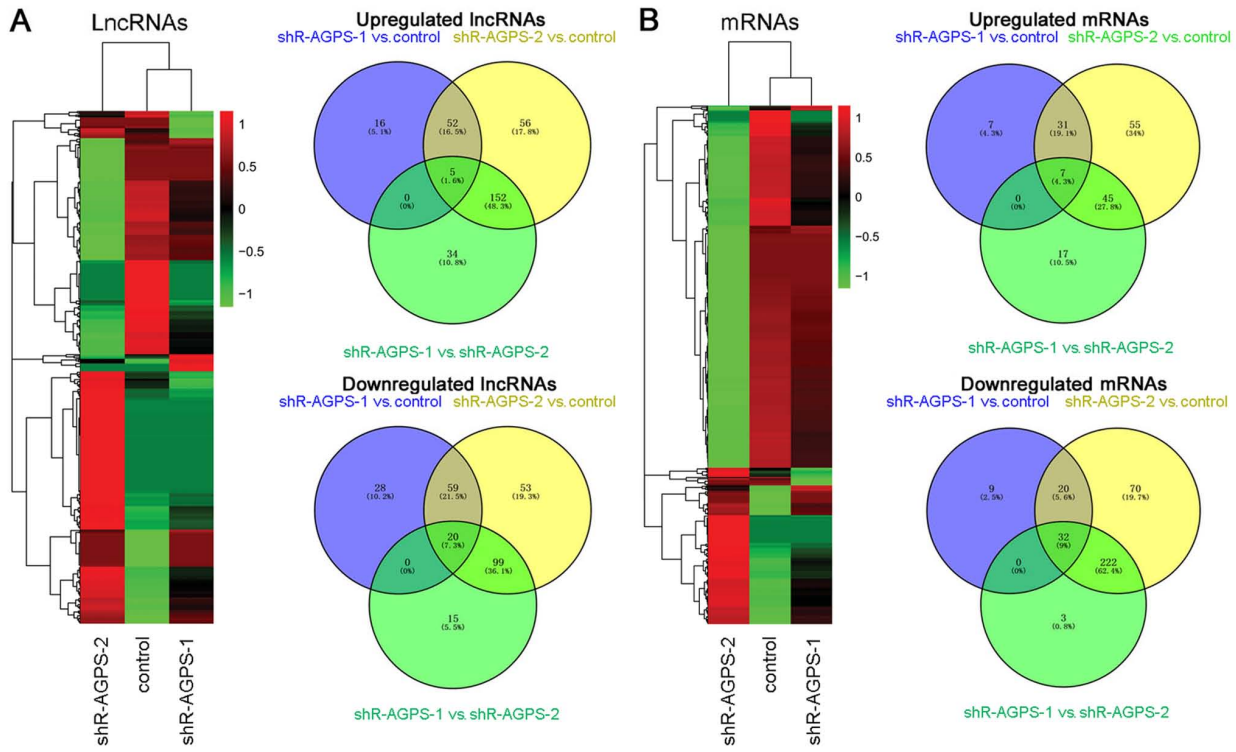

Figure 3. Distribution of differentially expressed lncRNAs and mRNAs identified in AGPS-silenced glioma cells. Heatmap and Venn diagrams of differentially expressed (A) lncRNAs and (B) mRNAs in AGPS-silenced U251 cells. The differential expression of lncRNAs and mRNAs were depicted in the heatmap. Green represents the downregulated expression of lncRNAs/mRNAs and red represents the upregulated expression of lncRNAs/mRNAs. The Venn diagrams represent the shared modified genes between groups. n=3. The scale bar indicates the FC, and (|FC|)>1.2 was used as a threshold. shR, short hairpin RNA; AGPS, alkylglycerone phosphate synthase; lncRNA, long non-coding RNA; FC, fold-change.

Table III. Top 40 differentially expressed mRNAs in AGPS-silenced human glioma U251 cells.

A, Top 40 differentially expressed mRNAs in the shR-AGPS-1 vs. control groups

mRNA	Upregulated FC	mRNA	Downregulated FC
OR2J2	1.84	CXCL8	2.10
THBS1	1.58	SLC7A11	1.81
KIR2DL5B	1.53	APOH	1.56
LTB	1.50	HMGA2	1.53
PRPS1	1.42	PSAT1	1.49
HIST1H3I	1.41	BLID	1.45
INTS4	1.35	ZNF404	1.44
RGCC	1.35	SLC38A1	1.43
MFAP4	1.34	CXCL8	1.43
KRT75	1.33	IGHD3-16	1.42
UNK	1.32	ZNF404	1.42
HES1	1.32	C3orf17	1.41
NQO1	1.30	CHML	1.41
FAIM2	1.30	IGFBP1	1.39
HIST1H4C	1.28	RPE 1.35	
KIR3DL2	1.28	OR2Z1	1.32
KRTAP5-3	1.27	SLC7A5	1.32
CCL2	1.27	DST 1.31	
HIST2H2AA4	1.26	PDK3	1.30
IGKV2-40	1.26	ASNS	1.30

B, Top 40 differentially expressed mRNAs in the shR-AGPS-2 vs. control groups

mRNA	Upregulated FC	mRNA	Downregulated FC
THBS1	2.31	CXCL8	6.94
PRPS1	1.89	AGPS	4.53
RGCC	1.79	IGFBP1	4.22
KRT75	1.71	APOH	3.22
NQO1	1.67	CXCL8	2.70
HIST1H3I	1.67	SLC7A11	2.67
KIR2DL5B	1.63	SLC38A1	2.45
CNN2	1.61	PTGS2	2.29
PLEKHA6	1.60	TREM1	2.28
IGKC	1.56	SCD	2.21
MFAP4	1.56	CHML	2.20
ITGA11	1.55	OGFRL1	2.16
OR10P1	1.51	IL7R	2.15
LTB	1.50	IGFBP3	2.12
TRDV1	1.46	SEL1L3	2.09
CCL2	1.46	HMGA2	2.06
DEPTOR	1.46	PSAT1	2.05
NOB1	1.45	DOCK10	2.03
C1QBP	1.43	ROS1	2.03
KRTAP10-10	1.42	PMAIP1	1.98

Table III. Continued.

C, Top 40 differentially expressed mRNAs in the shR-AGPS-1 vs. shR-AGPS-2 groups

mRNA	Upregulated FC	mRNA	Downregulated FC
THBS1	1.46	AGPS	3.55
IGHJ1	1.43	CXCL8	3.30
GPR33	1.38	IGFBP1	3.04
IGHD3-16	1.37	OR2J2	2.20
IGKC	1.34	APOH	2.06
KRTAP19-4	1.34	TREM1	1.90
PLEKHA6	1.34	SCD	1.90
EN2	1.33	CXCL8	1.89
BTNL2	1.33	IGFBP3	1.87
RGCC	1.33	PTGS2	1.84
PRPS1	1.32	OGFRL1	1.83
OR2Z1	1.32	SLC38A1	1.71
VN1R4	1.31	SEL1L3	1.70
OR10P1	1.30	STC1	1.70
ATOH8	1.30	ROS1	1.69
CNN2	1.30	IL7R	1.69
IGHV3OR16-9	1.30	SLC2A3	1.66
OR51B6	1.30	BDKRB1	1.65
DEPTOR	1.29	PANK3	1.63
KRT75	1.29	TXNIP	1.62

FC, fold change; shR, short hairpin RNA; AGPS, alkylglycerone phosphate synthase.

and 257 for shR-AGPS-1 vs. shR-AGPS-2) are represented in green, while the identified upregulated lncRNAs (73 for shR-AGPS-1 vs. control, 265 for shR-AGPS-2 vs. control, and 191 for shR-AGPS-1 vs. shR-AGPS-2) and mRNAs (45 for shR-AGPS-1 vs. control, 138 for shR-AGPS-2 vs. control, and 69 for shR-AGPS-1 vs. shR-AGPS-2) are represented in red, in AGPS-silenced and control glioma cells (Fig. 3A and B). Venn diagrams were used to compare the differentially regulated lncRNAs and mRNAs in the control, shR-AGPS-1 and shR-AGPS-2 groups. There were 57 and 79 lncRNAs shared between shR-AGPS-1 vs. control and shR-AGPS-2 vs. control, 5 and 20 shared between shR-AGPS-1 vs. control and shR-AGPS-1 vs. shR-AGPS-2, 157 and 119 shared between shR-AGPS-2 vs. control and shR-AGPS-1 vs. shR-AGPS-2, and 5 and 20 shared among all three groups for upregulated and downregulated lncRNAs, respectively; additionally, there were 38 and 52 mRNAs shared between shR-AGPS-1 vs. control and shR-AGPS-2 vs. control, 7 and 32 shared between shR-AGPS-1 vs. control and shR-AGPS-1 vs. shR-AGPS-2, 52 and 254 shared between shR-AGPS-2 vs. control and shR-AGPS-1 vs. shR-AGPS-2, and 7 and 32 shared among all three groups for upregulated and downregulated mRNAs, respectively (Fig. 3A and B). The top 40 differentially expressed lncRNAs and mRNAs, such as FOXF1 adjacent non-coding developmental regulatory RNA (FENDRR) and OR2J2 (which were upregulated compared with the control group), are presented in Tables II and III. RNAs with a (|FC|)>1.2 were upregulated or downregulated.

Functional prediction based on lncRNA and mRNA co-expression. According to the KEGG biological function analysis, the biological functions that were significantly enriched by differentially expressed genes were mainly involved in 'Human Diseases', 'Environmental Information Processing' and 'Organismal Systems' in biological systems. The biological functions that were significantly enriched by differential gene analysis were mainly involved in the 'Infectious diseases', Signal transduction' and 'Immune system' in cellular functions (Fig. 4A).

The co-expressed mRNAs identified in the present study were subjected to signaling pathway enrichment analysis by KEGG. It was identified that significantly enriched signaling pathways for the co-expressed mRNAs included the 'AGE-RAGE signaling pathway in diabetic complications', 'Rheumatoid arthritis', 'TNF signaling pathway', 'Protein processing in endoplasmic reticulum' and 'Malaria' (Fig. 4B).

GO enrichment BP analysis of the co-expressed lncRNAs and mRNAs indicated that the BPs of these two regulated types of RNA were associated with 'Cellular response to hypoxia', 'Extracellular matrix organization' and 'PERK-mediated unfolded protein response' (Fig. 4C); these functions are known to mediate protein responses, cell adhesion and the positive regulation of angiogenesis (12-14).

Construction of a signal transduction and pathway network from the co-expressed lncRNAs and mRNAs. Based on the

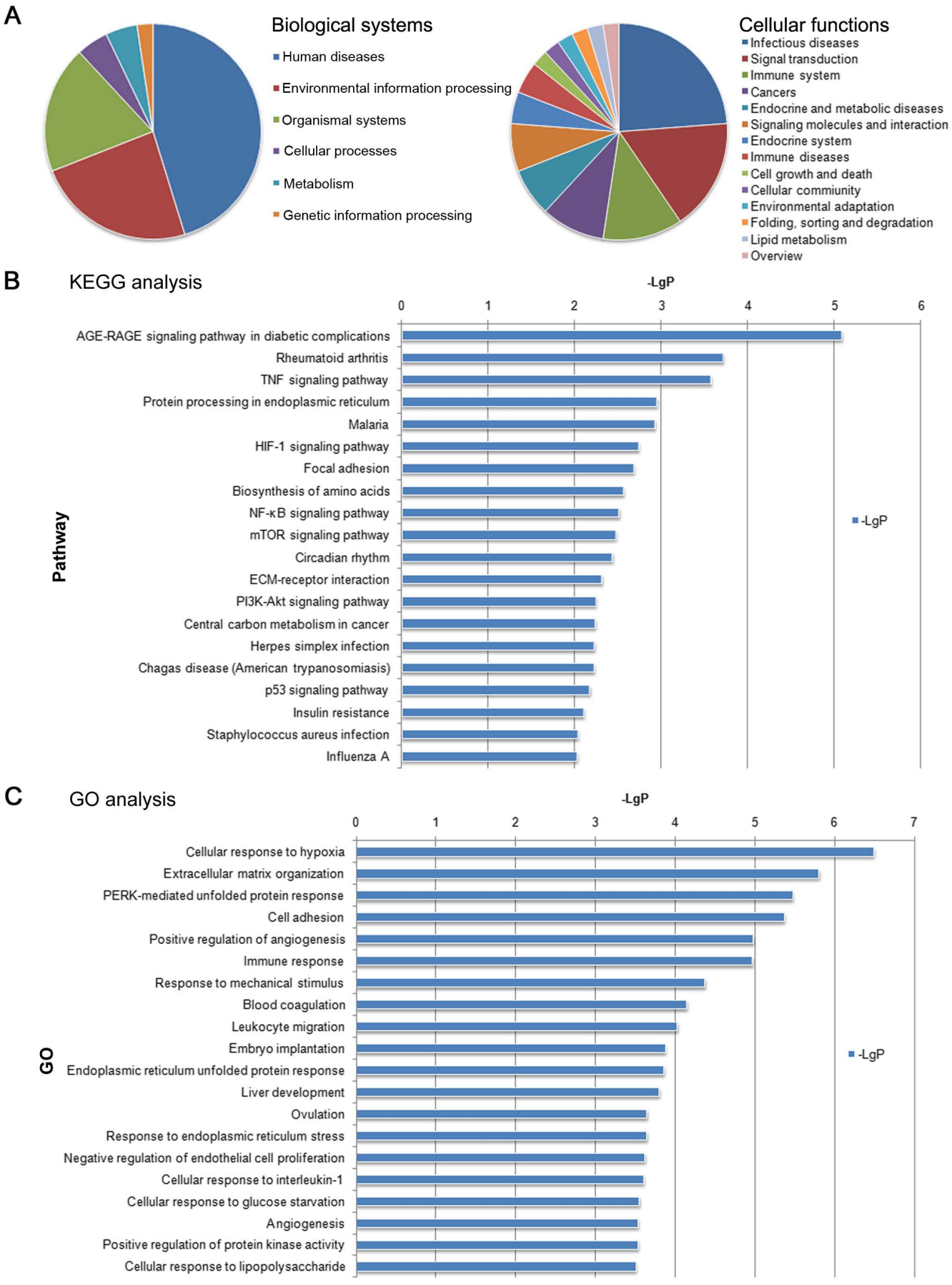

Figure 4. Functional prediction based on long non-coding RNA and mRNA co-expression in AGPS-silenced U251 cells. (A) Classification of KEGG biological functions analysis in AGPS-silenced glioma cells in Biological systems and Cellular functions. (B) Top 20 signaling pathways identified using KEGG signaling pathway enrichment analysis of AGPS-silenced U251 cells. (C) Top 20 biological process terms identified using GO enrichment analysis of AGPS-silenced U251 cells. AGPS, alkylglycerone phosphate synthase; KEGG, Kyoto Encyclopedia of Genes and Genomes; GO, Gene Ontology.

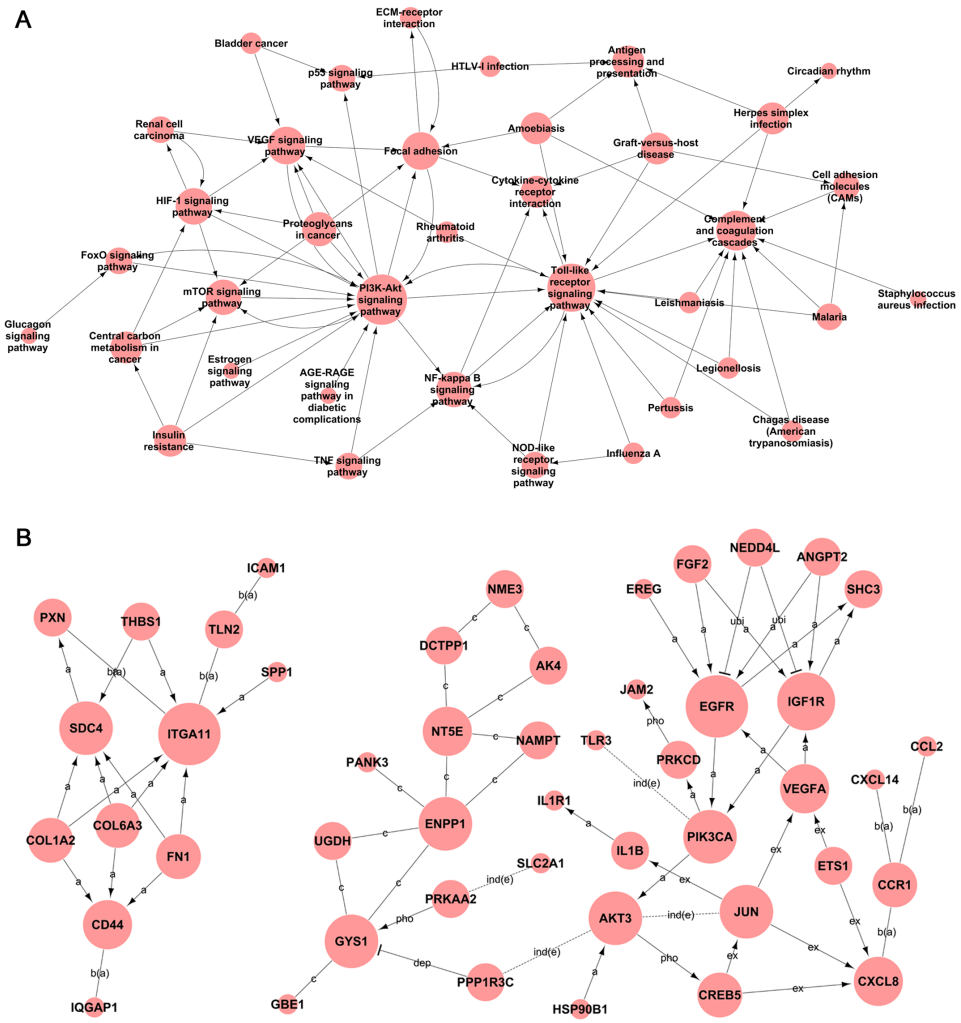

Figure 5. Signaling transduction and pathway network of co-expressed lncRNAs and mRNAs in AGPS-silenced U251 cells. (A) Pathway network of co-expressed lncRNAs and mRNAs in AGPS-silenced U251 cells. (B) Global signal transduction network of co-expressed lncRNAs and mRNAs in AGPS-silenced U251 cells. The nodes represent signaling pathways, lncRNAs and mRNAs and the arrows (or edges) represent the interaction/regulation between nodes. Ex, expression; pho, phosphorylation; a, activation; ind(e), indirect effect; b(a), binding/association; ubi, ubiquitination; dep, dephosphorylation; c, compound; s(c), state change; inh, inhibition; lncRNA, long non-coding RNA; AGPS, alkylglycerone phosphate synthase.

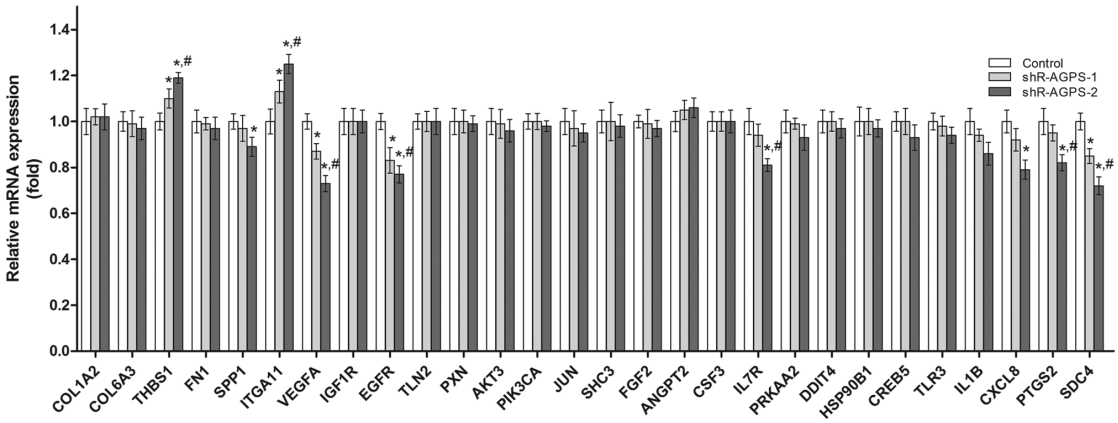

Figure 6. Effect of AGPS silencing on the expression levels of tumor-related mRNAs in glioma cells. Reverse transcription-quantitative PCR was used to analyze the mRNA expression levels of tumor-related mRNAs in AGPS-silenced U251 cells. *P<0.05 vs. control group; #P<0.05 vs. shR-AGPS-1 group. COL1A2, collagen I α2; COL6A3, collagen 6 α3; THBS1, thrombospondin-1; FN1, fibronectin 1; SPP1, secreted phosphoprotein 1; ITGA11, integrin subunit α11; VEGFA, vascular endothelial growth factor A; IGF1R, insulin-like growth factor 1 receptor; EGFR, epidermal growth factor receptor; TLN2, Talin 2; PXN, Paxillin; PIK3CA, phosphoinositide 3-kinase α; SHC3, Src homology 2 domain containing transforming protein 3; FGF2, fibroblast growth factor 2; ANGPT2, angiopoietin 2; CSF3, colony stimulating factor 3; IL-7R, interleukin-7 receptor subunit α; PRKAA2, protein kinase AMP-activated α2; DDIT4, DNA damage inducible transcript 4; HSP90B1, heat shock protein 90 kDa β1; CREB5, cyclic AMP-responsive element-binding protein 5; TLR3, Toll-like receptor 3; IL-1B, interleukin-1β; CXCL8, chemokine ligand 8; PTGS2, prostaglandin G/H synthase 2; SDC4, syndecan-4; shRNA, short hairpin RNA; AGPS, alkylglycerone phosphate synthase.

Table IV. Pathway networks in alkylglycerone phosphate synthase-silenced human glioma U251 cells.

Pathway name	Degree	Indegree	Outdegree
PI3K-Akt signaling pathway	19	12	7
Toll-like receptor signaling pathway	17	13	4
Complement and coagulation cascades	10	10	0
Focal adhesion	8	5	3
VEGF signaling pathway	8	6	2
HIF-1 signaling pathway	7	3	4
mTOR signaling pathway	6	5	1
NF-kappa B signaling pathway	6	4	2
Proteoglycans in cancer	5	0	5
Central carbon metabolism in cancer	4	1	3
Graft-versus-host disease	4	0	4
Antigen processing and presentation	4	4	0
Herpes simplex infection	4	0	4
Cytokine-cytokine receptor interaction	4	4	0
Amoebiasis	4	0	4
Insulin resistance	4	0	4
TNF signaling pathway	3	1	2
Renal cell carcinoma	3	1	2
Cell adhesion molecules	3	0	0
FoxO signaling pathway	3	2	1
Malaria	3	0	3
NOD-like receptor signaling pathway	3	1	2
p53 signaling pathway	3	3	0
Legionellosis	2	0	2
Pertussis	2	0	2
HTLV-I infection	2	0	2
ECM-receptor interaction	2	1	1
Influenza A	2	0	2
Leishmaniasis	2	0	2
Bladder cancer	2	0	2
Chagas disease (American trypanosomiasis)	2	0	0
Rheumatoid arthritis	2	0	2
AGE-RAGE signaling pathway in diabetic complications	1	0	1
Circadian rhythm	1	1	0
Glucagon signaling pathway	1	0	1
Staphylococcus aureus infection	1	0	1
Estrogen signaling pathway	1	0	1

signal transduction pathway interactions identified by KEGG signaling pathway enrichment analysis, a signaling pathway network was constructed using the OmicShare tools. The network consisted of 37 nodes and 158 connections. Amongst the most connected nodes identified was the PI3K-Akt signaling pathway, the Toll-like receptor signaling pathway, the complement and coagulation cascades, focal adhesion and the vascular endothelial growth factor (VEGF) signaling pathway (Fig. 5A). The analysis of the mRNAs corresponding to the signaling pathway action network was used to construct a global signal transduction network based on the interaction between genes, proteins and compounds, and to further obtain a network of interactions between mRNAs using the OmicShare tools. The network consisted of 75 nodes and 164 connections. The epidermal growth factor receptor (EGFR), integrin α-11 (ITGA11) and insulin-like growth factor 1 receptor (IGF1R) were the central sites in the pathway network (Fig. 5B).

Pathway network in AGPS-silenced human glioma cells. The pathway network in AGPS-silenced U251 cells is presented in Table IV. To further assess the expression levels and regulatory effect of AGPS on the pathway networks in human glioma cells, the mRNAs of important genes in the PI3K/Akt, Toll-like receptor, focal adhesion and VEGF signaling pathways were analyzed using RT-qPCR. Compared with the control cells, significantly upregulated expression levels of

thrombospondin-1 (THBS1) and ITGA11, and significantly downregulated expression levels of secreted phosphoprotein 1 (SPP1), VEGFA, EGFR, interleukin-7 receptor subunit α (IL7R), interleukin-8 (CXCL8), prostaglandin G/H synthase 2 (PTGS2) and syndecan-4 (SDC4), were identified in the shR-AGPS-transfected cells (Fig. 6).

lncRNA regulation pathway network. A lncRNA regulatory network was constructed using the OmicShare tools. Moreover, 979 connections were identified between the nodes. The Degree of the lncRNA and its target pathway was calculated by OmicShare tools 3.0 according to the connection around the lncRNA and its target pathway, and the more connections there were, the higher the Degree. Table V shows that the lncRNA with the highest Degree was AK093732. To analyze the importance of each pathway in the network, it was identified that the core signal transduction pathway regulated by differentially expressed lncRNAs was cytokine-cytokine receptor interaction (Fig. 7). The top 20 lncRNA-target pathway networks in AGPS-silenced U251 cells are presented in Table V.

Table V. Top 20 lncRNA-target pathway networks in alkylglycerone phosphate synthase-silenced U251 cells.

A, Pathway	Degree
Cytokine-cytokine receptor interaction	49
PI3K-Akt signaling pathway	45
Cell adhesion molecules (CAMs)	40
AGE-RAGE signaling pathway	36
p53 signaling pathway	36
Rheumatoid arthritis	36
NF-kappa B signaling pathway	34
Herpes simplex infection	33
Malaria	33
TNF signaling pathway	30
Glucagon signaling pathway	29
Focal adhesion	28
HTLV-I infection	28
Influenza A	27
Bladder cancer	26
Chagas disease (American trypanosomiasis)	26
Central carbon metabolism in cancer	25
Toll-like receptor signaling pathway	24
HIF-1 signaling pathway	22
Leishmaniasis	22

B, lncRNA	Degree
AK093732	34
LINC01384	27
FENDRR	25
uc011bsz.1	25
linc-PTPRN2	24
linc-U2AF1-1	24
RP11-221N13.3	24
BC042023	23
BC043357	23
linc_luo_1251	23
linc_luo_35	23
linc_luo_1223	22
LINC00973	22
linc-ANKRD20A1-20	22
linc-NBPF15-1	22
uc003flo.2	22
linc-ANKRD20A1-14	21
linc-DUSP10-7	21
linc-FOXB2-3	21
linc-WISP3-2	21

lncRNA, long non-coding RNA.

Discussion

AGPS is an enzyme that converts acylglycerol-3-phosphate to alkylglycerol-3-phosphate, which is a necessary step to generate all ether lipids (4). Cancer cells are known to metabolize lipids in a manner that is different from normal cells (15). In addition, the content of ether lipids in tumors has been discovered to be higher compared with healthy tissues (16). Moreover, the levels of ether lipids in malignant tumors were found to be increased compared with non-invasive tumors, and AGPS expression levels were also observed to be different in cancer cells (5-7). Tumorigenicity is known to be caused by invasive cancer cells (17), which is consistent with the present findings. In the present study, it was identified that, compared with the control group, AGPS silencing suppressed the proliferation of U251 cells.

The effect of AGPS on the pathway network was analyzed in human glioma cells by sequencing and bioinformatics analysis, and it was discovered that AGPS silencing regulated tumor-related signaling pathways, such as the PI3K/Akt, Toll-like receptor, focal adhesion and VEGF signaling pathways. These aforementioned results were further validated by RT-qPCR, where significantly upregulated expression levels of THBS1 and ITGA11, and downregulated expression levels of SPP1, VEGFA, EGFR, IL7R, CXCL8, PTGS2 and SDC4, were all identified; all of these are crucial genes involved in the aforementioned signaling pathways, and have been found to serve roles in tumor metastasis and angiogenesis (18-23).

lncRNAs were once considered to be a noisy byproduct of the transcription process (24). However, previous studies have reported that lncRNAs serve an important role at the RNA level in regulating cell proliferation, differentiation, the maintenance of pluripotent stem cells and cancer pathogenesis (25,26). The present study aimed to identify the lncRNAs associated with glioma, and subsequently used bioinformatics to analyze the biological functions and signal transduction pathways involved in the regulation of the lncRNAs identified. Furthermore, a regulatory network of lncRNAs in relation to signal transduction pathways was constructed to identify lncRNAs in a pivotal position. For example, FENDRR is an endothelial cell gene critical for vascular development, and it was previously reported that FENDRR overexpression

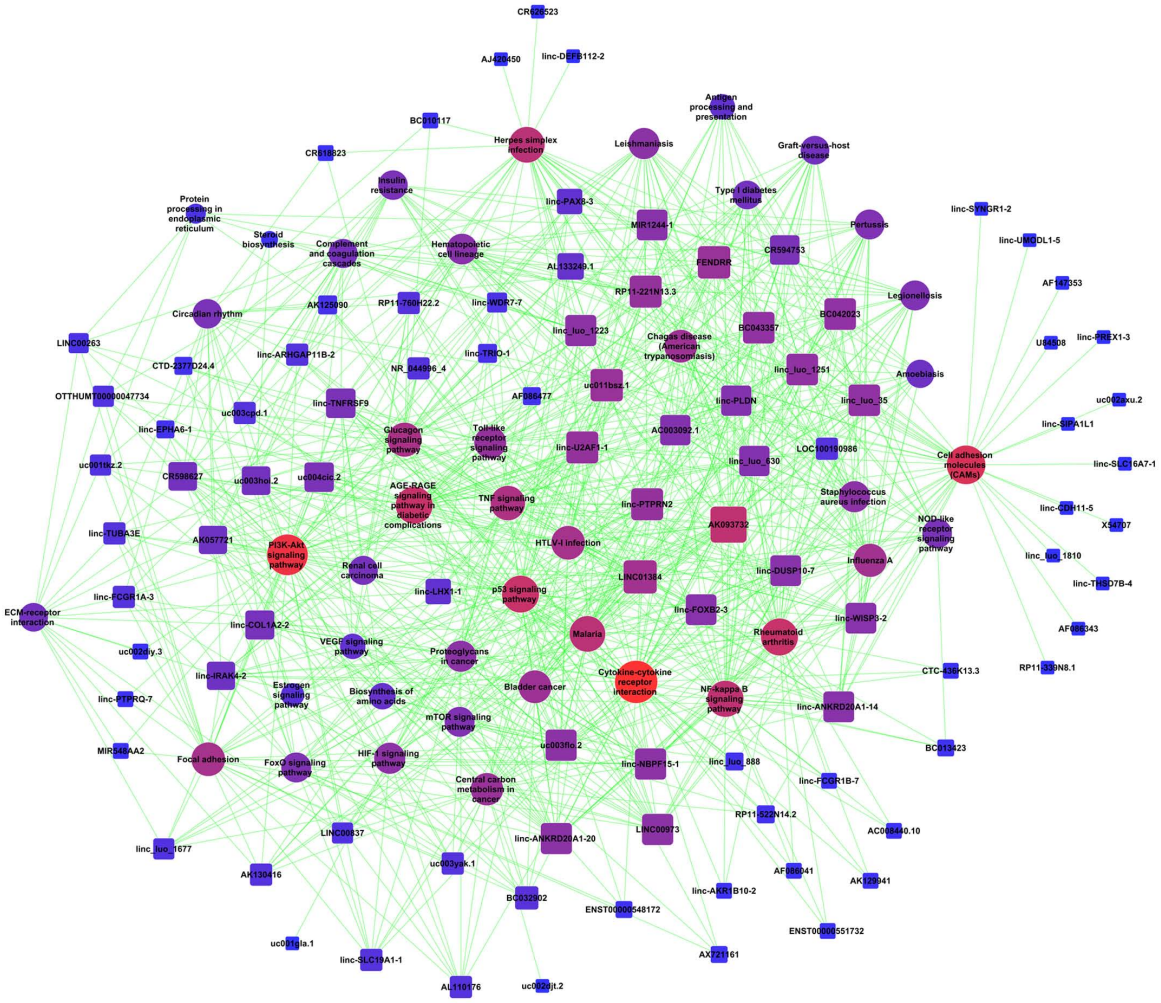

Figure 7. lncRNA target pathway network in AGPS-silenced U251 cells. The regulatory core pathways of differential lncRNAs were identified using a lncRNA-gene-pathway network, indicating the association between lncRNAs and pathways in AGPS-silenced glioma U251 cells. Red represents the higher Degree values, blue represents the lower Degree values and purple represents the middle Degree values. AGPS, alkylglycerone phosphate synthase; lncRNA, long non-coding RNA.

promoted the apoptosis of human brain microvascular endothelial cells (27). Other previous studies have also reported that FENDRR served an important regulatory role in numerous types of malignant tumor, such as human lung, colon, breast and liver cancer (28-30). For example, FENDRR reduced the stem cell characteristics of non-small cell lung cancer by inhibiting the ELAV-like protein 1/P-glycoprotein axis; and FENDRR was also discovered to inhibit Sox4 protein expression, which slowed the progression of colon cancer (31). However, to the best of our knowledge, there has been no previous research conducted on the role of FENDRR in glioma. In the present study, the expression levels of FENDRR in the AGPS-silenced groups were significantly upregulated compared with the control group, indicating that the expression levels of FENDRR may be negatively associated with the degree of glioma malignancy. However, the role of FENDRR in glioma cells and its related mechanisms requires further investigation.

It has been revealed that the expression levels of the lncRNA-PTPRN2 in the brains of mice treated with a neuroprotective preparation of trans-resveratrol were significantly downregulated compared with mice fed the standard diet (32). Notably, a previous study suggested that the lncRNA-PTPRN2, which had a pivotal position in the pathway regulatory network, may be involved in the regulation of cell adhesion molecules by regulating the expression levels of intercellular adhesion molecule-1 and signal transduction pathways, such as advanced glycation end products/receptor for advanced glycosylation end products, NF-κB and tumor necrosis factor (33). It was reported that also found that lncRNA AK093732 was an important site and highest Degree. In a previous study, lncRNA AK093732 was increased in laryngeal squamous cell carcinoma and considered a potential biomarker (34). However, further research is required to identify the regulatory mechanisms of PTPRN2 and AK093732 in these signaling pathways.

In conclusion, the present study analyzed the association and role of AGPS with the expression levels of lncRNAs and mRNAs in glioma. It was discovered that the identified differentially expressed lncRNAs and co-expressed mRNAs may serve important biological roles in the development, progression and metastasis of gliomas. Furthermore, the pathway networks identified also provide a reference and direction for further studies into the regulatory mechanisms of important lncRNAs in glioma and their associated signaling pathways.

Acknowledgements

Not applicable.

Funding

The present study was supported by the Special Program of Talent Development for Excellent Youth Scholars in Tianjin, China (grant no. TJTZJH-QNBJRC-2-9), the Natural Science Foundation of Tianjin (grant no. 16JCQNJC11500) and the Science and Technology Development Fund of Bengbu Medical College (grant no. BYKF1783).

Availability of data and materials

All data generated or analyzed during this study are included in this published article.

Authors' contributions

YZ was responsible for the conception and design of the study. LC and WZ were responsible for acquisition of data. LH and LJ were responsible for data interpretation. LQ was responsible for cellular and molecular experiments. All authors read and approved the final manuscript.

Ethics approval and consent to participate

Not applicable.

Patient consent for publication

Not applicable.

Competing interests

The authors declare that they have no competing interests.

References

1. Ferris SP, Hofmann JW, Solomon DA and Perry A: Characterization of gliomas: From morphology to molecules. Virchows Arch 2: 257-269, 2017.
2. Benjamin Daniel I, Cravatt Benjamin F and Nomura Daniel K: Global profiling strategies for mapping dysregulated metabolic pathways in cancer. Cell Metab 5: 565-577, 2012.
3. Piano V, Benjamin DI, Valente S, Nenci S, Marrocco B, Mai A, Aliverti A, Nomura DK and Mattevi A: Discovery of inhibitors for the ether lipid-generating enzyme AGPS as anti-cancer agents. ACS Chem Biol 11: 2589-2597, 2015.
4. Benjamin DI, Cozzo A, Ji X, Roberts LS, Louie SM, Mulvihill MM, Luo K and Nomura DK: Ether lipid generating enzyme AGPS alters the balance of structural and signaling lipids to fuel cancer pathogenicity. Proc Natl Acad Sci USA 110: 14912-14917, 2013.
5. Hou S, Tan J, Yang B, He L and Zhu Y: Effect of alkylglycerone phosphate synthase on the expression profile of circRNAs in the human thyroid cancer cell line FRO. Oncol Lett 15: 7889-7899, 2018.
6. Stazi G, Battistelli C, Piano V, Mazzone R, Marrocco B, Marchese S, Louie SM, Zwergel C, Antonini L, Patsilinakos A, *et al*: Development of alkyl glycerone phosphate synthase inhibitors: Structure-activity relationship and effects on ether lipids and epithelial-mesenchymal transition in cancer cells. Eur J Med Chem 163: 722-735, 2019.
7. Zhu Y, Zhu L, Lu L, Zhang L, Zhang G, Wang Q and Yang P: Role and mechanism of the alkylglycerone phosphate synthase in suppressing the invasion potential of human glioma and hepatic carcinoma cells *in vitro*. Oncol Rep 32: 431-436, 2014.
8. Jarroux J, Morillon A and Pinskaya M: History, discovery, and classification of lncRNAs. Adv Exp Med Biol 1008: 1-46, 2017.
9. Jiang X, Yan Y, Hu M, Chen X, Wang Y, Dai Y, Wu D, Wang Y, Zhuang Z and Xia H: Increased level of H19 long noncoding RNA promotes invasion, angiogenesis, and stemness of glioblastoma cells. J Neurosurg 2016: 129-136, 2016.
10. Lim W and Kim HS: Exosomes as therapeutic vehicles for cancer. Tissue Eng Regen Med 16: 213-223, 2019.
11. Livak KJ and Schmittgen TD: Analysis of relative gene expression data using real-time quantitative PCR and the 2(-Delta Delta C(T)) method. Methods 25: 402-408, 2001.
12. Noman MZ, Hasmim M, Messai Y, Terry S, Kieda C, Janji B and Chouaib S: Hypoxia: A key player in antitumor immune response. A review in the theme: Cellular responses to hypoxia. Am J Physiol Cell Physiol 309: C569-C579, 2015.
13. Pickup MW, Mouw JK and Weaver VM: The extracellular matrix modulates the hallmarks of cancer. EMBO Rep 15: 1243-1253, 2014.
14. Soni H, Bode J, Nguyen CDL, Puccio L, Neßling M, Piro RM, Bub J, Phillips E, Ahrends R, Eipper BA, *et al*: PERK-mediated expression of peptidylglycine α-amidating monooxygenase supports angiogenesis in glioblastoma. Oncogenesis 9: 18, 2020.
15. Wood R and Snyder F: Characterization and identification of glyceryl ether diesters present in tumor cells. J Lipid Res 8: 494-500, 1967.
16. Jaffrès PA, Gajate C, Bouchet AM, Couthon-Gourvès H, Chantôme A, Potier-Cartereau M, Besson P, Bougnoux P, Mollinedo F and Vandier C: Alkyl ether lipids, ion channels and lipid raft reorganization in cancer therapy. Pharmacol Ther 165: 114-131, 2016.
17. Li Y, Han X, Feng H and Han J: Long noncoding RNA OIP5-AS1 in cancer. Clin Chim Acta 499: 75-80, 2019.
18. Shen J, Cao B, Wang Y, Ma C, Zeng Z, Liu L, Li X, Tao D, Gong J and Xie D: Hippo component YAP promotes focal adhesion and tumour aggressiveness via transcriptionally activating THBS1/FAK signalling in breast cancer. J Exp Clin Cancer Res 37: 175, 2018.
19. Wu P, Wang Y, Wu Y, Jia Z, Song Y and Liang N: Expression and prognostic analyses of ITGA11, ITGB4 and ITGB8 in human non-small cell lung cancer. PeerJ 7: e8299, 2019.
20. Jeong BY, Cho KH, Jeong KJ, Park YY, Kim JM, Rha SY, Park CG, Mills GB, Cheong JH and Lee HY: Rab25 augments cancer cell invasiveness through a β1 integrin/EGFR/VEGF-A/Snail signaling axis and expression of fascin. Exp Mol Med 50: e435, 2018.
21. Zeng B, Zhou M, Wu H and Xiong Z: SPP1 promotes ovarian cancer progression via Integrin β1/FAK/AKT signaling pathway. Onco Targets Ther 11: 1333-1343, 2018.
22. Rhead B, Shao X, Quach H, Ghai P, Barcellos LF and Bowcock AM: Global expression and CpG methylation analysis of primary endothelial cells before and after TNFa stimulation reveals gene modules enriched in inflammatory and infectious diseases and associated DMRs. PLoS One 15: e0230884, 2020.
23. Ni M, Liu X, Meng Z, Liu S, Jia S, Liu Y, Zhou W, Wu J, Zhang J, Guo S, *et al*: A bioinformatics investigation into the pharmacological mechanisms of javanica oil emulsion injection in non-small cell lung cancer based on network pharmacology methodologies. BMC Complement Med Ther 20: 174, 2020.
24. Long Y, Wang X, Youmans DT and Cech TR: How do lncRNAs regulate transcription? Sci Adv 3: eaao2110, 2017.
25. Abedini P, Fattahi A, Agah S, Talebi A, Beygi AH, Amini SM, Mirzaei A and Akbari A: Expression analysis of circulating plasma long noncoding RNAs in colorectal cancer: The relevance of lncRNAs ATB and CCAT1 as potential clinical hallmarks. J Cell Physiol 234: 22028-22033, 2019.
26. Liang WC, Ren JL, Wong CW, Chan SO, Waye MM, Fu WM and Zhang JF: LncRNA-NEF antagonized epithelial to mesenchymal transition and cancer metastasis via cis-regulating FOXA2 and inactivating Wnt/β-catenin signaling. Oncogene 37: 1445-1456, 2018.
27. Wang B, Xian J, Zang J, Xiao L, Li Y, Sha M and Shen M: Long non-coding RNA FENDRR inhibits proliferation and invasion of hepatocellular carcinoma by down-regulating glypican-3 expression. Biochem Biophys Res Commun 509: 143-147, 2019.
28. Zhang G, Han G, Zhang X, Yu Q, Li Z, Li Z and Li J: Long non-coding RNA FENDRR reduces prostate cancer malignancy by competitively binding miR-18a-5p with RUNX1. Biomarkers 23: 435-445, 2018.

29. Liu J and Du W: LncRNA FENDRR attenuates colon cancer progression by repression of SOX4 protein. Onco Targets Ther 12: 4287-4295, 2019; Li Y, Zhang W, Liu P, Xu Y, Tang L, Chen W and Guan X: Long non-coding RNA FENDRR inhibits cell proliferation and is associated with good prognosis in breast cancer. Onco Targets Ther 11: 1403-1412, 2018.
30. Xu R and Han Y: Long non-coding RNA FOXF1 adjacent non-coding developmental regulatory RNA inhibits growth and chemotherapy resistance in non-small cell lung cancer. Arch Med Sci 15: 1539-1546, 2019.
31. Gong F, Dong D, Zhang T and Xu W: Long non-coding RNA FENDRR attenuates the stemness of non-small cell lung cancer cells via decreasing multidrug resistance gene 1 (MDR1) expression through competitively binding with RNA binding protein HuR. Eur J Pharmacol 853: 345-352, 2019.
32. Navarro G, Martínez-Pinilla E, Sánchez-Melgar A, Ortiz R, Noé V, Martín M, Ciudad C and Franco R: A genomics approach identifies selective effects of trans-resveratrol in cerebral cortex neuron and glia gene expression. PLoS One 12: e0176067, 2017.
33. Lee EJ, Rath P, Liu J, Ryu D, Pei L, Noonepalle SK, Shull AY, Feng Q, Litofsky NS, Miller DC, *et al*: Identification of global DNA methylation signatures in glioblastoma-derived cancer stem cells. J Genet Genomics 42: 355-371, 2015.
34. Shen Z, Li Q, Deng H, Lu D, Song H and Guo J: Long non-coding RNA profiling in laryngeal squamous cell carcinoma and its clinical significance: Potential biomarkers for LSCC. PLoS One 9: e108237, 2014.